ELSEVIER

Surface and Coatings Technology 126 (2000) 181–194

SURFACE & COATINGS TECHNOLOGY

www.elsevier.nl/locate/surfcoat

Scratch–wear resistance of nanoscale super thin carbon nitride overcoat evaluated by AFM with a diamond tip

Mingwu Bai[a,*], Koji Kato[a], Noritsugu Umehara[a], Yoshihiko Miyake[b], Junguo Xu[c], Hiromitsu Tokisue[c]

[a] *Department of Mechanical Engineering, Tohoku University, Sendai 980-8579, Japan*
[b] *Data Storage and Retrieval System Division, Hitachi Ltd., Odawara 256-8510, Japan*
[c] *Mechanical Engineering Research Laboratory, Hitachi Ltd., Ibaraki 300-0013, Japan*

Received 23 August 1999; accepted in revised form 24 November 1999

Abstract

Atomic force microscopy (AFM) was used to investigate the scratch–wear resistance of ultrathin superhard carbon nitride overcoats of thickness 1, 2, 4, 6, 8 and 10 nm. When sliding against a diamond tip of radius less than 100 nm in the mode of line scratch, the thin overcoats of thickness 1–4 nm exhibited poor wear resistance, especially at contact pressures larger than 25 GPa, with a wear depth of 4 nm or larger and a specific wear rate up to 0.8×10^{-4} mm^3/nm. Non-contact mode imaging of a scratched surface has shown that a large amount of nanoscale wear debris was formed along the two sides of the scratched grooves, which indicated that the material removal mechanism of such thin overcoats was due to brittle fracture and abrasive wear, both in the nanoscale. In comparison, the overcoats of thickness 6–10 nm exhibited wear resistance with a specific wear rate less than 0.2×10^{-4} mm^3/nm. Instead, the least debris was observed on the scratched surfaces and only shallow grooves were left after scratching. It means that the grooves were formed by both plough and plastic deformation. The micro/nanowear mechanism and thickness effect of coating on scratch resistance were discussed.

Keywords: Scratch; Carbon nitride; Coating; Thickness; Wear

1. Introduction

In order to increase the storage capacity of magnetic recording systems, the hard disk drive industry is focusing on reducing the flying height between the magnetic head slider and the disk. Area density in magnetic storage is now increasing at a fast pace of 45–65% annually. According to this trend, the thickness of the thin coating on the hard disk, currently 10–12 nm, will decrease furthermore, without sacrificing performance to satisfy the increasing market demand. It is necessary to understand the nanoscale mechanical and tribological characteristics of the very thin coating for both practical and scientific significance. Because the friction and wear behavior in the lightly loaded head–disk interface is mainly controlled by both physical and chemical properties of a few surface atomic layers, it is applicable to use a diamond tip with an applied load within the range of micronewtons in AFM to simulate the contact situation which is similar to those which occur in head–disk interfaces.

Since Binnig et al. [1] developed the atomic force microscope (AFM) several researchers have modified the AFM to investigate microtribological characteristics of the thin coating. Mate et al. [2] measured the atomic friction of a tungsten tip sliding on a basal

* Corresponding author. Fax: +81-22-217-6955.
E-mail address: mbai@tribo.mech.tohoku.ac.jp (M. Bai)

0257-8972/00/$ - see front matter
PII: S0257-8972(99)00656-8

plane of a graphite surface. Kaneko et al. [3] investigated the microscopic friction force on magnetic media and head sliders by a friction force microscope (FFM), they [4] also developed a point contact microscope to evaluate the nanotribological properties of the thin coating. Most recently, using similar experimental means, Wei and Komvopoulos [5] investigated the wear characteristics of smooth ultrathin coating of hydrogenated carbon with thicknesses of 5, 10 and 25 nm; Anoikin et al. [6] compared the nanowear properties of various carbon coatings of 5–10 nm. Although they have obtained valuable information about properties of thin coating, much work still needs to be done for understanding the thickness effect and contact stress effect on the nanoscale scratch–wear properties, and especially for clarifying the material removal mechanism of extremely thin coating.

In this study, we used a diamond tipped pin sliding against a nanoscale thin CN_x coating to evaluate the thin coating's macro/nano scratch–wear resistance and to identify the thinnest CN_x coating which still exhibits good wear resistance. An AFM operating in the lateral (friction) force mode (LFM) was also used to study micro/nanotribological properties of nanoscale carbon nitride overcoats during scratch tests. Identification of friction characterization and wear morphology in combination with finite element analysis (FEA) was used to clarify micro/nanowear mechanisms and to explain the thickness effect of the coating on scratch resistance.

2. Experimental method

2.1. Preparation of materials

Amorphous carbon nitride coating was prepared by the ion beam assisted deposition (IBAD) method [7]. Before deposition, the vacuum chamber was evacuated to 1×10^{-6} Torr and the working pressure was maintained at approximately 1×10^{-4} Torr. Silicon (111) substrate was sputter-cleaned prior to deposition by a 5-min bombardment with N^+. The amorphous carbon nitride coatings were synthesized by mixing sputtered carbon and energetic N^+. Sputtered carbon was formed by sputtering graphite (> 99.999% purity) with Ar under an energy of 1 KeV and a current of 100 mA. Energetic N^+ was produced under the energy and current of 1.0 KeV, 20 $\mu A/cm^2$. The deposition rate of carbon which was monitored via a calibrated quartz crystal oscillator was 2.0 nm/min, after calibration by step masked coatings. Ultra thin carbon nitride (CN_x) overcoats with thicknesses ranging from 1 to 10 nm were synthesized. The atomic concentration of nitrogen in amorphous CN_x is approximately 11% according to analysis by X-ray photoelectron spectroscopy. The surface roughness of the CN_x coating was measured by a commercial AFM (Seiko Instruments Inc., SP13700 + SPA300). The roughness of arithmetic average (Ra), root-mean-square deviation (R_{rms}), and 10-point average (Pz), all in nanometer units, are all listed in Table 1. The images of surface morphology (not shown here) indicate that only 1-nm CN_x coatings inherit the surface morphology of the silicon substrate.

Table 1
Surface roughness of CN_x coating with different thickness

Thickness (nm)	0	1	2	4	6	8	10
Roughness (nm)							
Ra	0.11	0.32	0.25	0.41	0.18	0.17	0.20
RMS	0.14	0.55	0.31	0.50	0.23	0.22	0.25
Pz	1.91	2.29	2.17	2.62	1.64	1.34	1.94

Raman spectroscope with an Ar ion laser (12 mA) was used to characterize the overcoat structure. The reference laser wavelength was 514.5 nm. The laser spot size was approximately 1 μm, and the acquisition time was 500 s. No big difference in Raman spectra between different coatings was found. Fig. 1 shows a typical micro-Raman spectra of the carbon nitride coating with a thickness of 10 nm. The peak at approximately 1540 cm^{-1} (G band) overlapped with a broad band at approximately 1350 cm^{-1} (D band) is indicated by two arrows. The G band corresponds to graphite-like layers of sp^2 microdomains in the coating, while the D band is attributed to bond angle disorder in the graphite-like microdomains induced by the linking with sp^3 carbon atoms as well as the finite crystalline sizes of sp^2 microdomains in the coating [8]. The large intensity ratio (I_D/I_G) between the D band and G band can be attributed to the scratch resistance of the CN_x coating. Since it is difficult to measure the hardness of a thin coating with a thickness less than 10 nm due to substrate effect, the hardness of CN_x was measured on a thick coating, which was fabricated by the same synthesis parameters except deposition time. The hardness of a CN_x coating with a thickness of 100 nm was measured by a nanoindentation tester (NEC MHA-400) with a load of 0–0.5 mN and indentation speed of 2.7 nm/s, the averaged hardness is approximately 22.0 GPa.

2.2. Experimental method

AFM with a diamond-tipped stainless steel cantilever was used to scratch the CN_x coating [6]. The diamond tip is a three-sided pyramid with an apex angle of 80° and an end-tip nominal radius of approximately 100 nm. The calibration of the spring constants of the AFM cantilevers was carried out in a commercial nanoindentation tester by deflecting the cantilevers under pre-set loads. During friction curve measurement, the tip slided against the coating in a reciprocal sliding

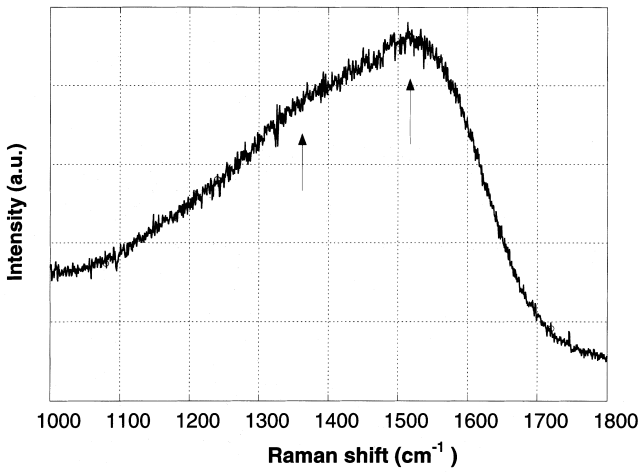

Fig. 1. A typical micro-Raman spectra of the carbon nitride films with thickness of 10 nm. The peak at approximately 1540 cm^{-1} (G-peak) overlapped with a broad band at approximately 1350 cm^{-1} (D-peak) is indicated by arrows.

mode in one cycle. At least five duplicated tests were conducted and averaged values were reported. No pre-scanning was setup to let the tip slide against an absolute non-worn surface, because pre-scanning, as setup as for a default operation procedure, may result in a scanning wear of 0.1–0.5 nm or larger, even at the lowest reference force in AFM. During the scratch test, unidirectional reciprocal sliding mode was used because the slider head in the hard disk drive works in this mode. The programmed step includes: approaching the diamond tip to the surface with no load; loading to a preset load; unidirectional line scratching with a distance of 1000 nm; unloading; moving back to the original starting site; duplicate above operation by changing loads or scratch cycles according to programmed input list. Every scratch cycle was delayed for 2 min to relax elastic deformation formed during the scratch process. The tip slided against the coating with pre-set force with a sliding velocity of 0.25 nm/s and an applied load of 1, 10, 15, 25, 35 and 45 μN, respectively, which corresponded to an initial maximum Hertzian pressure of 8.6, 18.4, 21.1, 25.0, 28.0 and 30.4 GPa, respectively. After the scratch tests, the wear morphology was imaged by the same tip but under the lowest load. A scanning wear, which is formed during imaging by scanning a selected area, although is very small, was also measured and was considered in plotting the figures of wear depth vs. applied load. Triplicate tests or more were conducted and average values were reported here, the relative errors of the tests were indicated in the figures. All experiments were performed in ambient conditions (25°C, 40–60% RH) and the instrument was kept in a sound-proof hood.

The applied load was decided by the following equation [9]: $W = W_{\mathrm{fr}} + W_{\mathrm{dif}} = W_{\mathrm{fr}} + kN_{\mathrm{dif}}/S$ where W_{fr} is the load according to preset reference force in the AFM operation, W_{dif} is the extra load in consideration of the contribution of the differentiate signal from the vertical two quadrants of the photodiode detector (N_{dif}) in AFM [10], k is the cantilever stiffness, and S is the sensitivity of AFM. The values of W_{fr}, S, and N_{dif} were measured before the AFM experiment, and k was measured by a nanoindentation. The friction force (mv) can be transferred as a friction coefficient according to the following calculation [9]:

$$F_n = \frac{K_t \cdot d_t \cdot H_{\mathrm{tip}}}{\alpha_{\mathrm{sensitivity}} \cdot 10^6 \cdot 2.5 \cdot L_{\mathrm{cantilever}}}$$

where F_n is friction force in Newton units, K_t is the twisted stiffness of the cantilever in units of N/m, d_t is the measured voltage in units of mV, H_{tip} is the height of the diamond tip in units of μm, L is the length of cantilever, $\alpha_{\mathrm{sensitivity}}$ is the vertical sensitivity of the diamond tipped cantilever in units of mV/nm. The value of K_t was supplied by the cantilever manufacturer, values of d_t, H_{tip}, and $L_{\mathrm{cantilever}}$ were measured before the AFM experiment by an optical microscope, and $\alpha_{\mathrm{sensitivity}}$ was obtained during the AFM experiment. The measured friction force was comparable to published references [5,10,13].

3. Results and discussion

3.1. Scratch–wear tests

Wear depth of CN_x coating as a function of coating thickness is presented in Fig. 2. A 45° slope line is introduced in the figure to show whether the wear occurred in the CN_x coating or in the substrate, e.g. whether wear depth is greater than or less than the thickness of CN_x coating. It is seen that 1 nm, 2 nm and 4 nm CN_x, especially for the coating with a thickness of 1 nm, exhibited very poor wear resistance, especially at high contact pressure. The wear depth of these three kinds of coating were between 2 and 14 nm, which was far greater than their coating thickness, it means that the wear mainly occurred in the silicon substrate, so the wear depth was large, as a result of swift wearing and depletion of coated coatings. For the coating with thickness ranging from 6 to 10 nm, they exhibited significant wear resistance. The wear depth was all less than 3.6 nm, far from their corresponding coating thickness. It means that in this experimental condition of applied loads ranging from 1 to 45 μN and maximum Hertzian contact pressures ranging from 8.6 to 30.4 GPa, the CN_x coating of thickness from 6 to 10 nm had an antiscratch effect. Interestingly, even for the CN_x coating with a thickness of 1–2 nm, then can

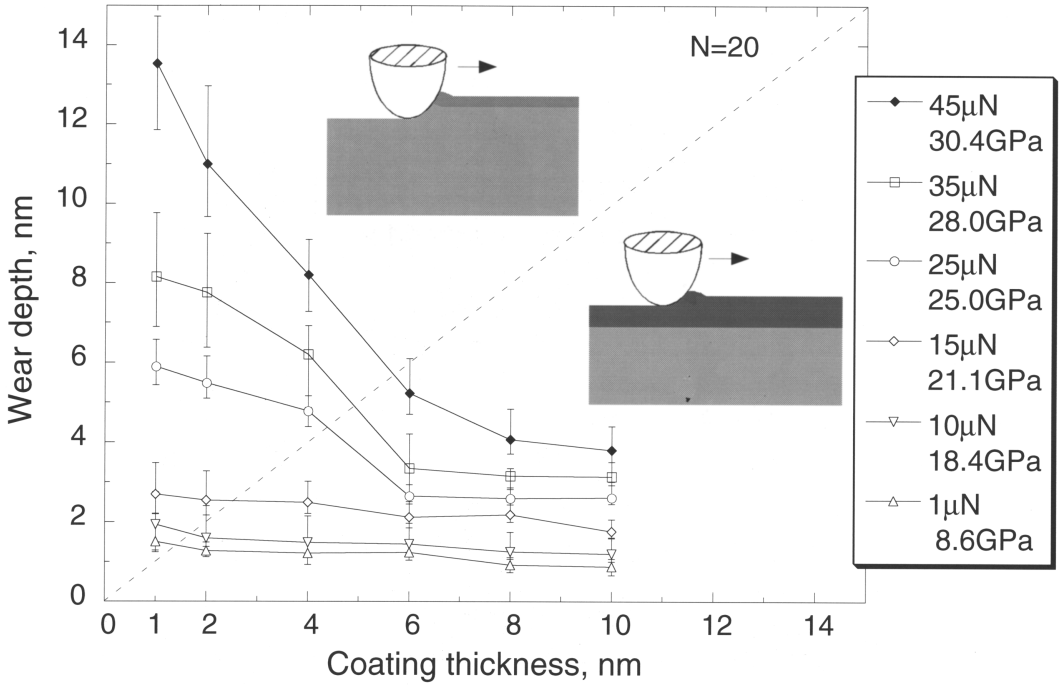

Fig. 2. Wear depth of the CN_x overcoat on silicon substrate as a function of CN_x coating thickness under different applied loads and maximum initial contact pressures.

exhibit scratch resistance as long as the applied load is low enough.

From the point of view of material characterization, some pin-holes may exist during the synthesis process in the 1- and 2-nm coating and so the coating would be non-homogeneous and so they would exhibit poor wear resistance, because they decreased the strength and hardness of the coating [11]. In addition, because both the interface strength and bonding strength of all coatings are almost the same due to adoption of the same synthesis conditions and process parameters except deposition time (assuming the internal stress in all the

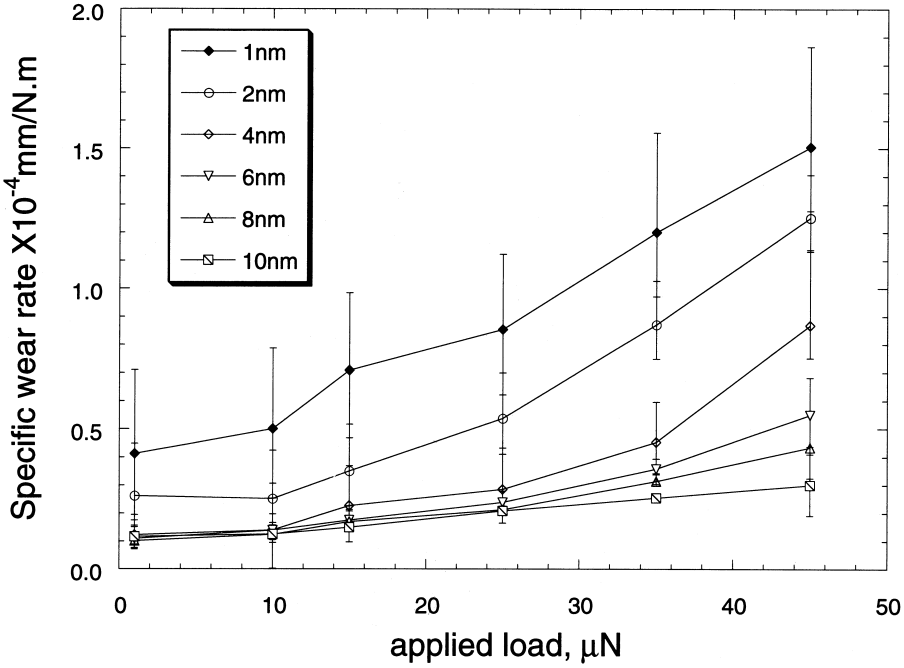

Fig. 3. Specific wear rate of CN_x coatings as a function of initial maximum contact pressure for the coating with thickness ranging from 1 to 10 nm. The applied loads were 1, 10, 15, 25, 35 and 40 μN, respectively.

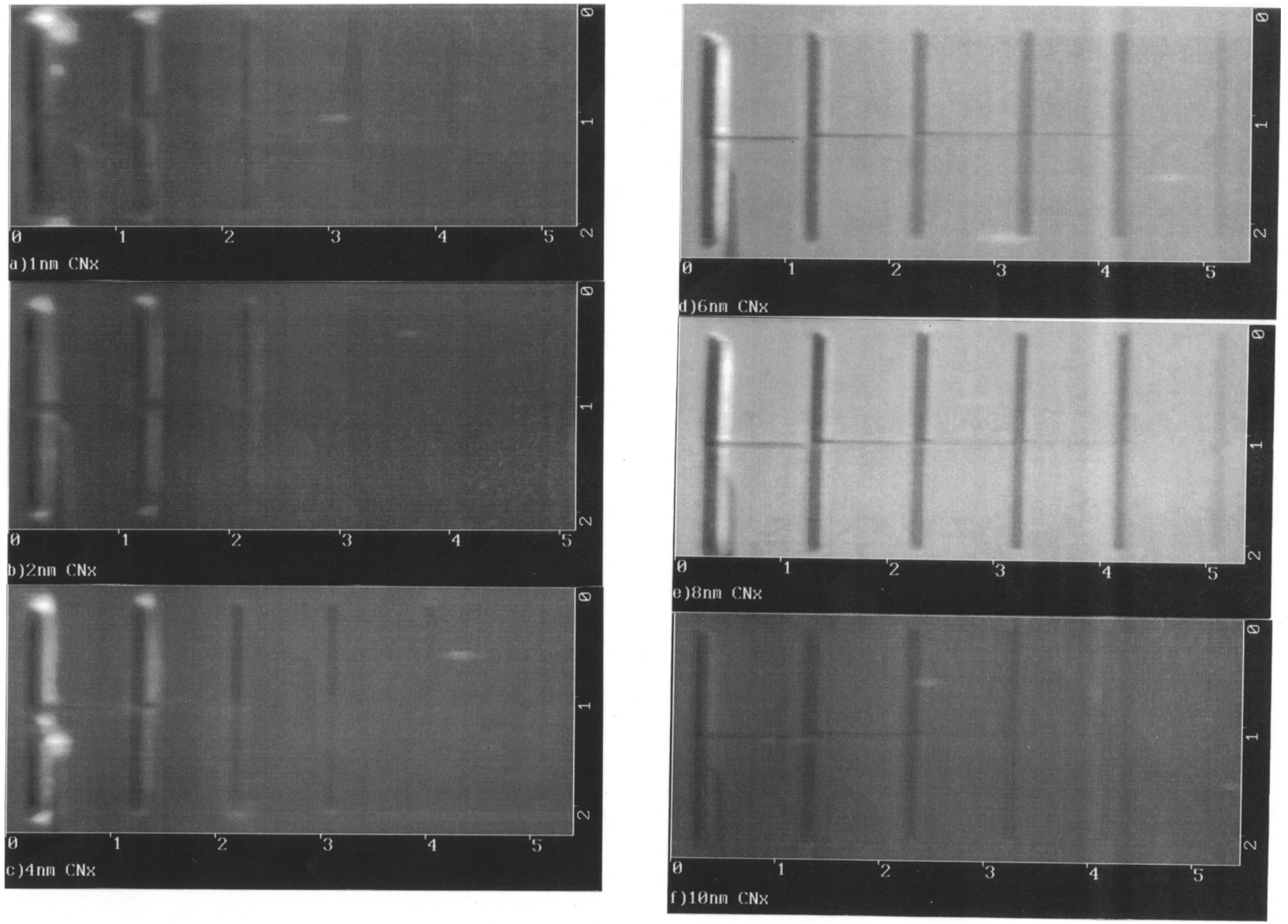

Fig. 4. AFM contact mode images and two-dimensional surface profiles of scratched surfaces of CN_x coatings with thicknesses of (a) 1 nm; (b); 2 nm; (c) 4 nm; (d) 6 nm; (e) 8 nm; and (f) 10 nm, respectively. The applied loads were (from right to left) 1, 10, 15, 25, 35 and 40 μN, respectively. Note that the depth scale of the profiles are different from one to another.

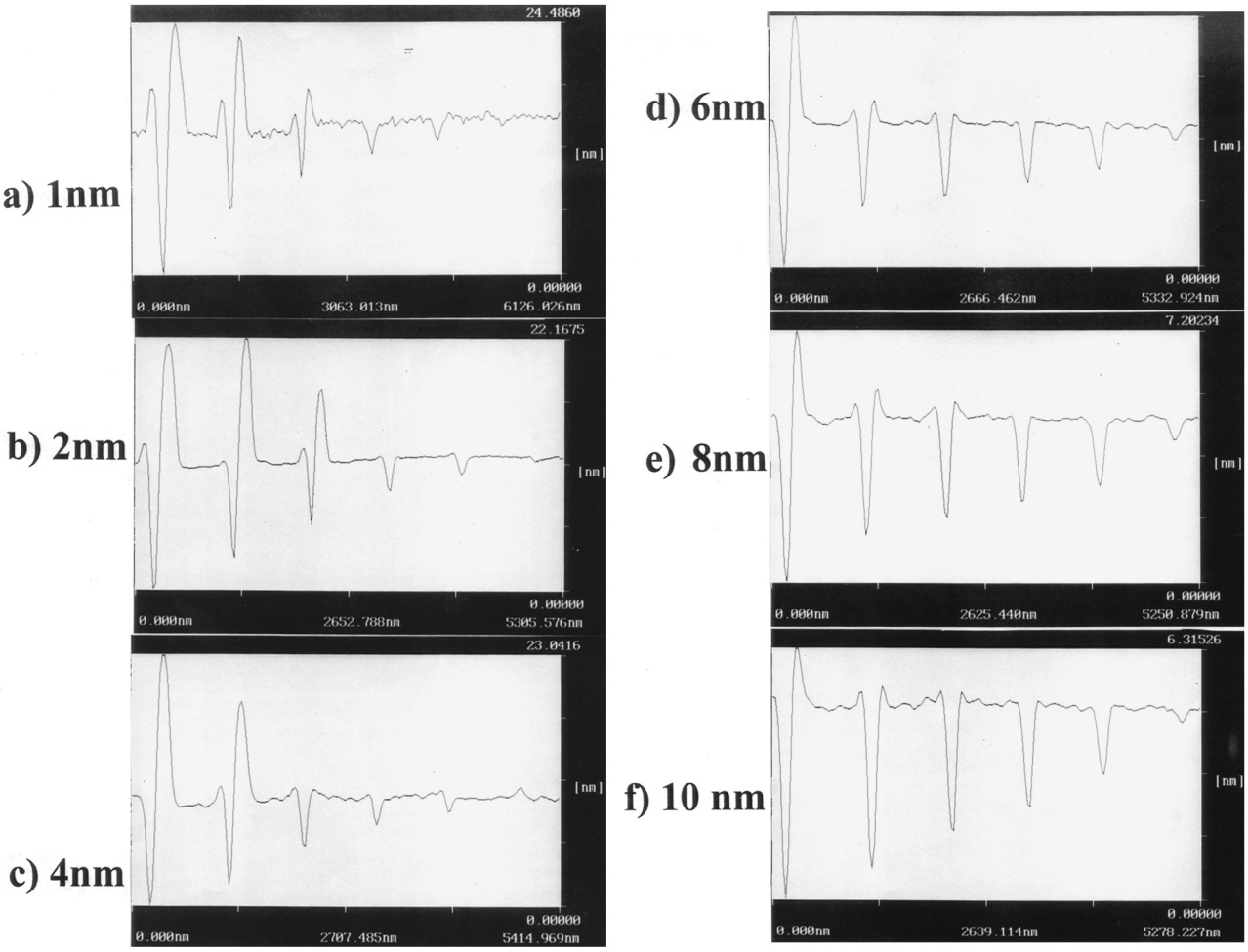

Fig. 4. (*Continued*)

coating are neglectably small [12]), a possible reason for the better wear resistance of the 'thick' coating can be attributed to the thickness effect.

A program was written to calculate the area of cross-section of every wear groove, and then the averaged wear rate of the coating was obtained. Fig. 3 shows the wear rate of various coatings as a function of maximum contact pressure. With increasing applied loads, the wear rate of the 1-, 2-, and 4-nm CN_x coatings increased at a large slope, while the wear rate of the other three kinds of coating showed a slow increase. This is because, for the coating with a thickness of 1–4 nm, the wear occurred in 'thin' CN_x only at the initial stage and mainly in the 'soft' silicon substrate during most of the time of the scratch process especially at severe contact pressure, hence the curve also reflects the poor wear-resistance of silicon substrate, i.e. cracks were easily initiated and swiftly propagated in single-crystal silicon subsurface especially under large contact pressures [13] when it slided against the diamond tip. In comparison, with increasing applied loads, the wear rate of the CN_x coating with a thickness from 6 to 10 nm increased very slowly, because the wear completely occurred in the CN_x coating, and their better wear resistance prevented them from quickly wearing.

Fig. 4 shows wear images of worn CN_x surfaces and typical cross-section profiles, it is deserved to mention that the depth scale of profiles shown in the right-up of the figure is different from other profiles. These images were obtained by in-situ scanning of scratched surfaces by the same diamond pin. The horizontal scratched line in the middle position of the images was formed due to high wedge blocking the movement of the diamond tip when it transferred its scratch track from one to another. It was found from the figure that high wedge was formed after scratching especially for the CN_x coating with the thickness of 1–6 nm at higher contact pressures. Almost no wear debris was seen on the worn surfaces because the stainless steel cantilever has large stiffness and it pushed away the wear debris from the worn area during line-by-line scanning. Furthermore, in-situ imaging resulted in slight wearing during scanning imaging (here we call it 'scanning wear'), even at

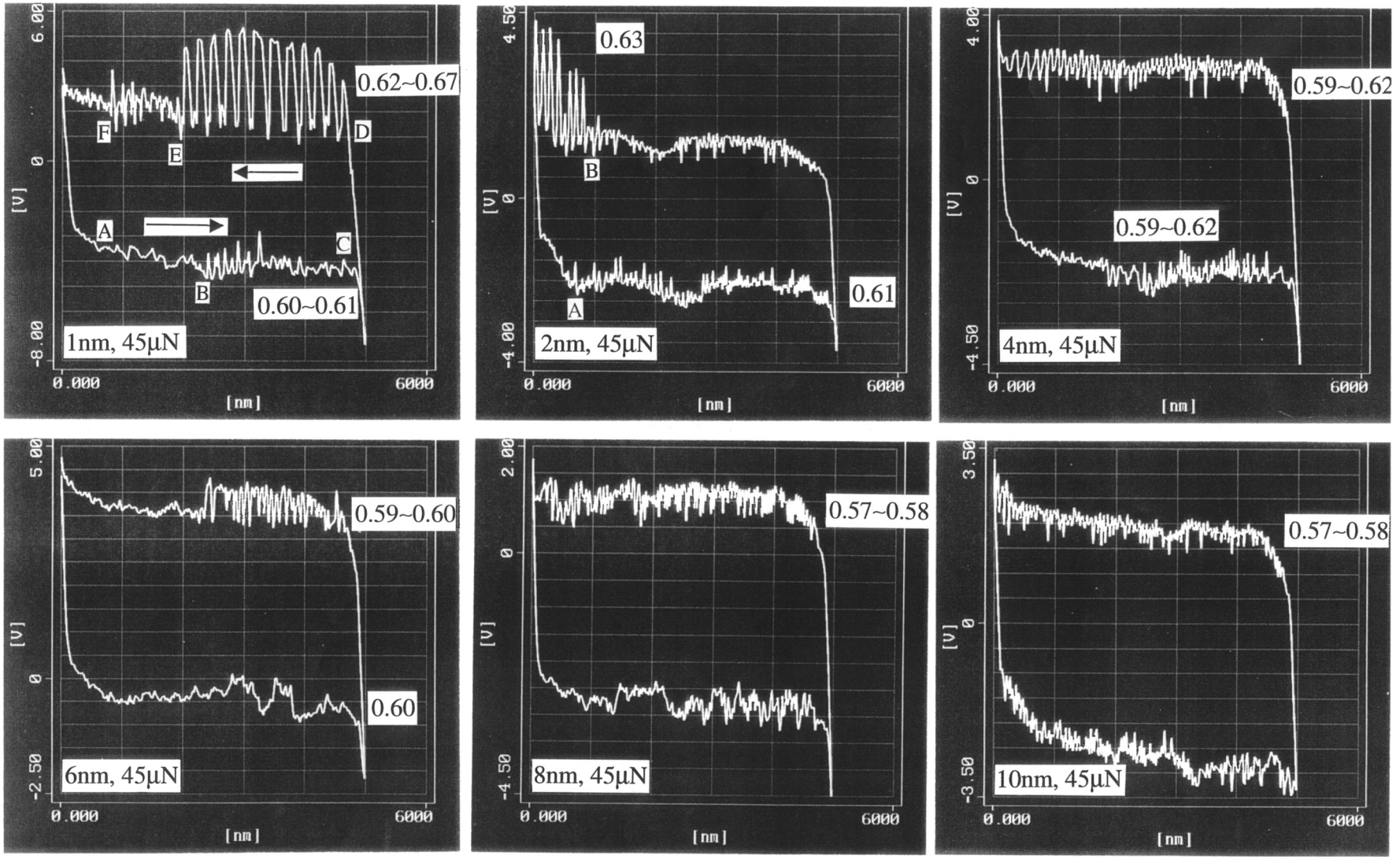

Fig. 5. Friction force (coefficient) as a function of sliding distance when the diamond pin slided against the CN_x coating in one reciprocal sliding cycle.

the lowest controllable loads. Therefore, the worn surfaces were smooth and free of debris. A non-contact imaging method, which is known as tapping mode [14], was also used to image the morphology of wear morphology especially of debris, which will be discussed later in this paper.

3.2. Friction results

The friction force vs. sliding distance curve in one scratch cycle was obtained by Friction Force Microscopy (FFM) [15]. No pre-scan was adopted to prevent any surface damage due to selection of the imaging center and the scanning area by pre-scanning. Fig. 5 shows the friction force as a function of sliding distance when the diamond tip slides against CN_x in one sliding cycle (2×5000 nm) under the applied load of 45 μN. When the applied load was very low, 1 μN, the friction coefficient was very low and was approximately 0.12 or so and it did not change too much with an increase in the applied loads. In addition, the friction was stable and no large friction fluctuation was observed. When the applied load increased to 10 μN, the friction coefficient increased to 0.22–0.24, and there was a little friction fluctuation in the case of CN_x with a thickness of 1 and 2 nm. Furthermore, increasing the applied load to 45 μN (Fig. 5), the maximum applied load in this experiment, there was a large friction fluctuation for the CN_x of 1- and 2-nm thickness. From Fig. 5a, in the forward cycle, the friction coefficient was between 0.60 and 0.61, when the diamond tip was in the way of return, the friction coefficient increased sharply (Fig. 5a, marked by D and E) and was between 0.62 and 0.67. It indicated that the thin coating partially cracked in the way between position B and C (in Fig. 5a, bottom) and the thin coating finally completely depleted or cracked in its returning way (marked by D and E). When the coating thickness increased to 2 and 4 nm, there was also a friction fluctuation and some sharp fluctuation, e.g. position B in Fig. 5b. When the coating thickness increased to 6–10 nm, no large or sharp friction fluctuation was encountered. From the friction force (coefficient) vs. sliding distance curves in Fig. 5, it may be deduced that coating cracking and formation of wear debris (observed by the non-contact mode) were mainly responsible for the large friction fluctuation of the 1 nm coating. On the other hand, differences in the rheological properties as a function of thickness were also responsible for the large friction fluctuation of the coating.

When the diamond pin slided against the silicon substrate, the in-situ-formed silicon oxides play the role of inhibiting adhesion between the diamond pin and silicon, as reported also by some researchers [16] that silicon exhibited negative wear due to in-situ-formed silicon oxides, hence a relatively low friction coefficient was observed. For a 1-nm thickness coating, because it is too thin and a pin-hole [17] may exist somewhere in the CN_x overcoat, its friction coefficient was a little high in comparison with that when the diamond slided against a silicon substrate. Another possible reason is that the 1-nm thickness coating had a low wear resistance and some in-situ formed debris including silicon oxides decreased the friction coefficient. For the coating with 2-nm thickness, a large friction coefficient was observed. This is because the coating with 2-nm thickness has a poor interface strength, and an interface partially debonding results in a large friction fluctuation. Because the friction between the diamond pin and the coating is less than that between the diamond pin and the silicon substrate, the friction coefficient increased when the diamond pin contacted the silicon surface after thin coating cracking and/or removal, meanwhile the friction fluctuation also increased clearly. AFM has a resolution of 0.1–0.5 nm in both the vertical and horizontal direction, it is supposed that the measured friction fluctuation was related to the initiation and propagation of cracks and/or to the formation of wear debris [18,19]. This was partly supported by real time observation in AFM, the abrupt increase in the friction signal always occurred in the place where the diamond tip scratched across a groove or debris which was ex-situ observed by non-contact mode imaging.

3.3. Wear morphology and wear mechanisms

The nanowear mechanisms had been investigated in different hard carbon coatings [5,17,21], however, the wear debris was not mentioned in these references [20] due to the limitation of instrument resolution and stability or other reasons, although wear debris is very important to clarify the material removal mechanism of thin coating. As discussed ahead, the AFM images in Fig. 4 were obtained by in-situ scanning using the same diamond tip for clearly worn morphology due to free debris. To clarify the wear mechanism of CN_x sliding against the diamond tip, an in-situ non-contact mode AFM imaging method was utilized instead of a conventional contact mode [6,21].

Fig. 6 shows the non-contact mode AFM images of the scratched CN_x surface. For the CN_x of 1-nm thickness sliding against the diamond tip in one cycle, a large amount of ribbon-like wear debris formed along the two sides of the wear grooves. The larger the applied load, the greater the wear debris. At the lowest applied load, 4 μN, only a small amount of wear debris was found, and meanwhile, a shallow groove was also seen clearly. The groove was formed partly due to plastic deformation of 1-nm thin coating and its substrate. Fig. 6b shows a two-dimensional cross-section profile of the scratch surface. Very high (~ 5–20 nm) peaks of two sides of the grooves indicate that a large

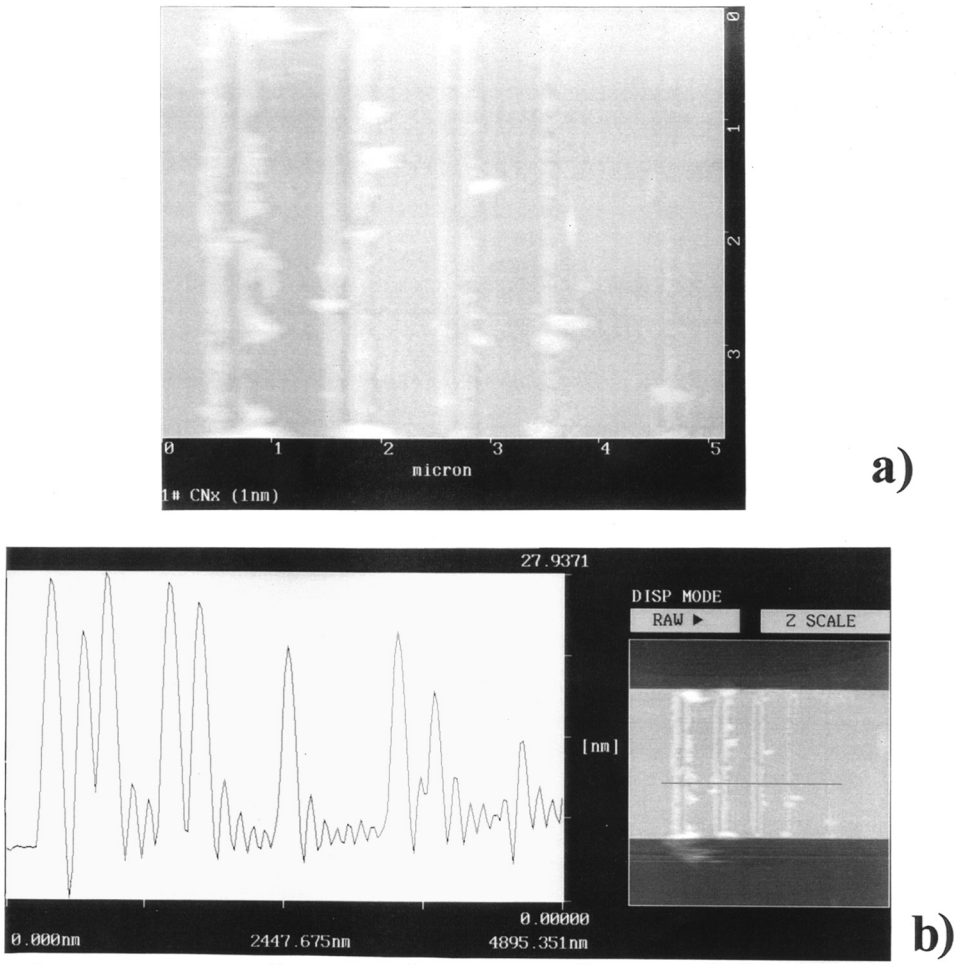

Fig. 6. Non-contact mode AFM image of the scratched CN_x surface. The CN_x of 1-nm thickness slided against the diamond tipped pin in one sliding cycle under applied loads (grooves from left to right) 45, 35, 25, 15, and 10 μN, respectively. (a) Top view image; and (b) two-dimensional profile of the cross-section.

amount of debris was agglomerated. The height of the debris peak was much larger than the depth of the wear groove, it means that the wear debris was loosely packed due to fracture of the peeled coating after scratching. The above phenomena demonstrates that the material removal mechanism of 1-nm coating was ploughing, cutting, and brittle fracture, all in nanoscale. The observed wear mechanism was different with wear mechanism observed in sub-micro scale in which in-situ SEM was used to identify the wear mechanism of the diamond pin (radius ~ 27 μm) sliding against stainless steel at an applied load of approximately 0.35 N [22].

With increasing CN_x overcoat thickness to 2 nm (Fig. 7a), the amount of wear debris was decreased. With thickness of the CN_x overcoat increased to 6–10 nm, the worn morphology and wear debris is completely different. Fig. 8 shows a typical AFM image of the scratched CN_x surface obtained by in-situ non-contact mode. The amount of wear debris decreased significantly, and the wear debris was thin plate-like and was formed mainly by the plough mode. The wear mechanism was delamination as discussed in another paper [11,13]. On the other hand, 1-nm CN_x exhibited poor wear resistance because it may have contained a pinhole which decreased its strength and hardness [11].

For 1 nm overcoats, a large amount of wear debris was seen on the nearby sides of wear grooves, the probable reason is that the hard ultra-thin coating was easily cracked and smashed into pieces easily. The phenomena may be used to explain why large friction fluctuation occurred for ultra-thin coating such as 1-nm coating, as shown in Fig. 5. The build-up and trapping of third-bodies in the sliding interface due to interface cracking results in large fluctuation of vanishing thin coating, however, for very thin coating of thickness 6 nm or thicker, the friction force in plough components was small, which corresponded to lower friction [23].

As a result, there are two types of wear debris found in this study. Agglomerated continuous ribbon-like debris (Figs. 6 and 7) indicated that thin CN_x exhibited poor scratch resistance and low fracture strength, especially under high contact pressure (25–35 GPa). An-

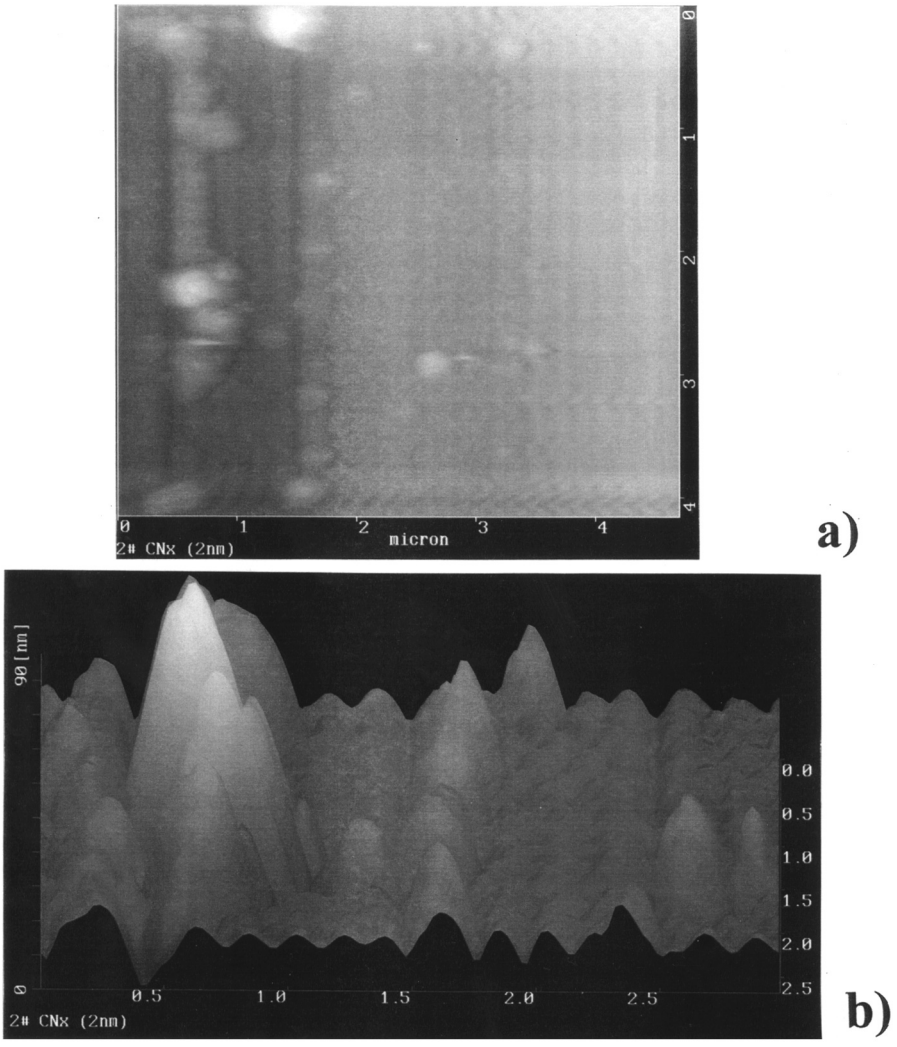

Fig. 7. Non-contact mode AFM image of the scratched CN_x surface. The CN_x of 2-nm thickness slided against the diamond tipped pin in one sliding cycle under applied loads (grooves from left to right) 45, 35, 25, 15, and 10 μN, respectively. (a) Top view image; and (b) three-dimensional morphology.

other debris type is plate-like debris (Fig. 8), which was formed due to plough in nanoscale, mainly occurred in the coating with thickness over 6 nm.

Wei et al. [5] and Kulkarni et al. [24] have investigated the nanowear properties of thin carbon coating with thicknesses of 10 and 20 nm, they found that there existed a critical load, below the critical load no significant wear was observed. However, such phenomenon was not observed in other studies [4,17,25,31]. In this study, a very clear critical load was not found for all of the CN_x coating with thicknesses of 1, 2, 4, 6, 8 and 10 nm when they slided against the diamond pin under a wide range of applied loads from 1 to 45 μN. Interestingly, in this investigation, there existed a dependence of wear resistance on coating thickness, in other words, a critical coating thickness of 4–6 nm existed, below this thickness, large wear and friction was observed. As analyzed before, it was probably that it was too thin to resist scratch wear, and the extreme thin coating was poorly bonded to its substrate due to existence of the pin-hole and material non-homogeneity.

FEM has been successfully extended to model nanoscale contact mechanics in recent years [26,29]. In this study, three-dimensional elastic–plastic finite element analysis was used to calculate the stress distribution on CN_x coatings and its substrate when the CN_x coating slid against diamond pin under different applied loads. During FEM calculation, the diamond indenter was modeled with Young's elastic modulus, $E = 1140$ GPa and Poisson's ratio, $\nu = 0.07$ [27]. The carbon nitride coating was modeled with $E = 200$ GPa according to the measurement results of nanoindentation and $\nu = 0.25$. Work hardening was fixed at zero for all calculations since the amorphous carbon nitride is not expected to show hardening behavior. According to the

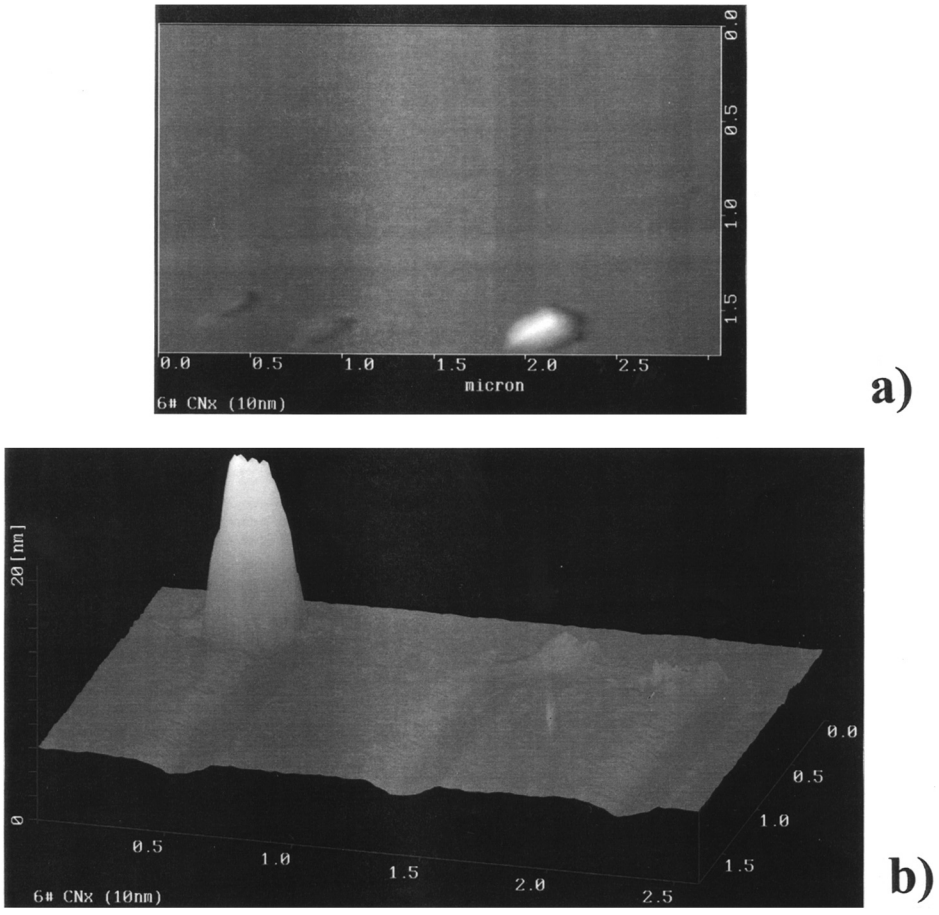

Fig. 8. Non-contact mode AFM image of the scratched CN_x surface. The CN_x of 10-nm thickness slided against the diamond tipped pin in one sliding cycle under applied loads (grooves from left to right) 45, 35, 25, 15, and 10 μN, respectively. (a) Top view; and (b) three-dimensional morphology.

measurement of the friction coefficient in this experiment, the friction coefficient was selected as 0.1, 0.2, and 0.6, respectively when the applied loads were 1, 10, and 45 μN, respectively. The maximum shear stress is supposed to result in material failure by the process of crack initiation and propagation [28] According to von Mises yield criterion [29], the propensity for yielding in the coating and substrate is governed by:

$J_2 = 1/6\{(\sigma_1 - \sigma_2)^2 + (\sigma_2 - \sigma_3)^2 + (\sigma_3 - \sigma_1)^2\}$ in which σ_1, σ_2 and σ_3 are the principal stresses in the state of complex stress [30]. Typical contour plots of J_2 are shown in Fig. 10 for the CN_x overcoats of 10-nm thickness sliding against the diamond pin under different applied loads. At a low applied load of 1 μN, the maximum von Mises stress is 8.377 GPa (Fig. 10), and its position was in the substrate of the coating. Hence, the cracks were most probably initiated at first at this position and propagated toward the surface. Mild wear mode, delamination, dominated in the scratch process. When the applied load was increased to 10 μN, the maximum von Mises stress moved to the surface and the value also increased to 22.65 GPa, near the hardness of the carbon nitride coating, so it results in a quick wear, and the wear mode is most probably a mix of mild delamination and plough. For the largest applied load of this test, 45 μN, the maximum von Mises stress is 76.09 GPa, which is much more larger than the hardness of the coating, so it results in severe wear of coating, which is due to plough or abrasion. In comparison, in the case of the coating with thickness of 1 nm (their stress contour is not given here), the maximum von Mises stresses are as large as 44 GPa (10 μN) and 106 GPa (45 μN), far greater than the hardness of the coating (22 GPa), and their position are all in the surface. The surface layer could be removed very easily under such high stress, this is in agreement with the results in the scratch test. Hence the main wear mechanism was micro/nano-cutting, accompanied by large plastic deformation. It should be pointed out that, these calculation results here are just to show the trends of stress distribution because the FEM modelling did not consider crack initiation, crack propagation and debris formation, and in fact, the actually stress could not arrive so high, this is because before it

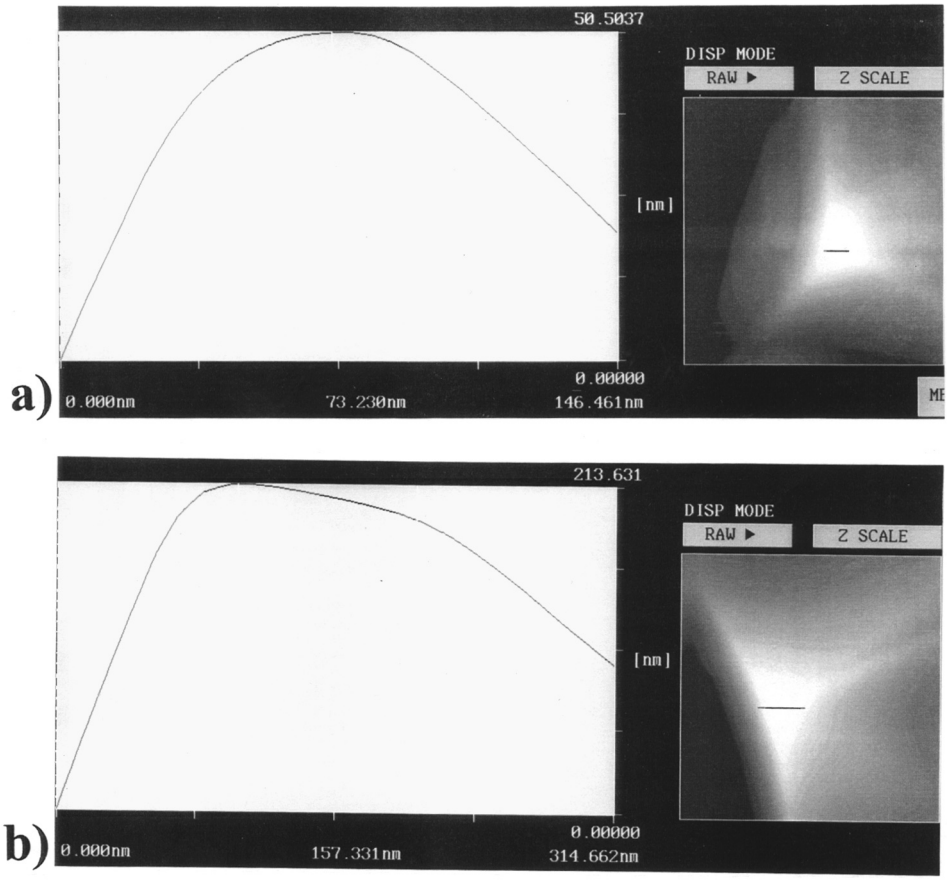

Fig. 9. Contact mode images of the diamond tip scanned by an Si_3N_4 tip. (a) Before scratch; and (b) after scratch.

arrives to the FEA calculated value, the thin film was already scratched away very easily under such severe loading conditions.

3.4. Wear of diamond tips

The wear of the diamond pin was checked by imaging the diamond tip by another more sharp Si_3N_4 tip (tip radius $\sim$5–20 nm) in AFM (Fig. 9). Typically, from Fig. 9a, the unworn diamond tip was very sharp and with good roundness in the top tip. After one turn scratch test with a 10 nm CN_x overcoat, minor wear can be found in Fig. 9b. In comparison of wear of the CN_x coating, the wear of the diamond tip was very small, it can be attributed to the adoption of the line-scratch mode and low sliding speed, instead of the area-scratch mode [4–6,31], and on the other hand, the diamond tip is harder than CN_x.

4. Conclusions

The scratch–wear resistance of the CN_x coating with thickness ranging from 1 to 10 nm slid against diamond tip under contact pressures of 8.6–30.4 GPa was investigated in AFM. Based on experimental results and analysis, it was concluded that the wear resistance of CN_x was sensitive to both the applied load and film thickness. There existed a critical CN_x coating thickness which decides different wear rate and wear mechanism: (1) When the applied load was greater than 25 μN, the critical coating thickness was 6 nm. Below this critical thickness, CN_x had large wear depth especially for the case of 1–2-nm thickness in which a large amount of wear debris was found near the two sides of scratch grooves, the wear mechanism was nanoscale cutting, abrasion and brittle fracture, the wear occurred mainly in substrate; while above this critical thickness, CN_x had a low wear depth especially for the case of 8–10-nm thickness, almost no wear debris was found, the wear mechanism was micro/nano plough, accompanied by large plastic deformation, the wear occurred in the CN_x film. (2) When the applied load was less than 15 μN, the critical coating thickness was approximately 2 nm. Above this critical thickness, the wear occurred in CN_x; and below this critical thickness, the wear mainly occurred in the substrate. It means that even extremely thin CN_x, e.g. 2-nm CN_x, can exhibit wear resistance as long as the applied load was low enough, e.g. 10 μN or lower.

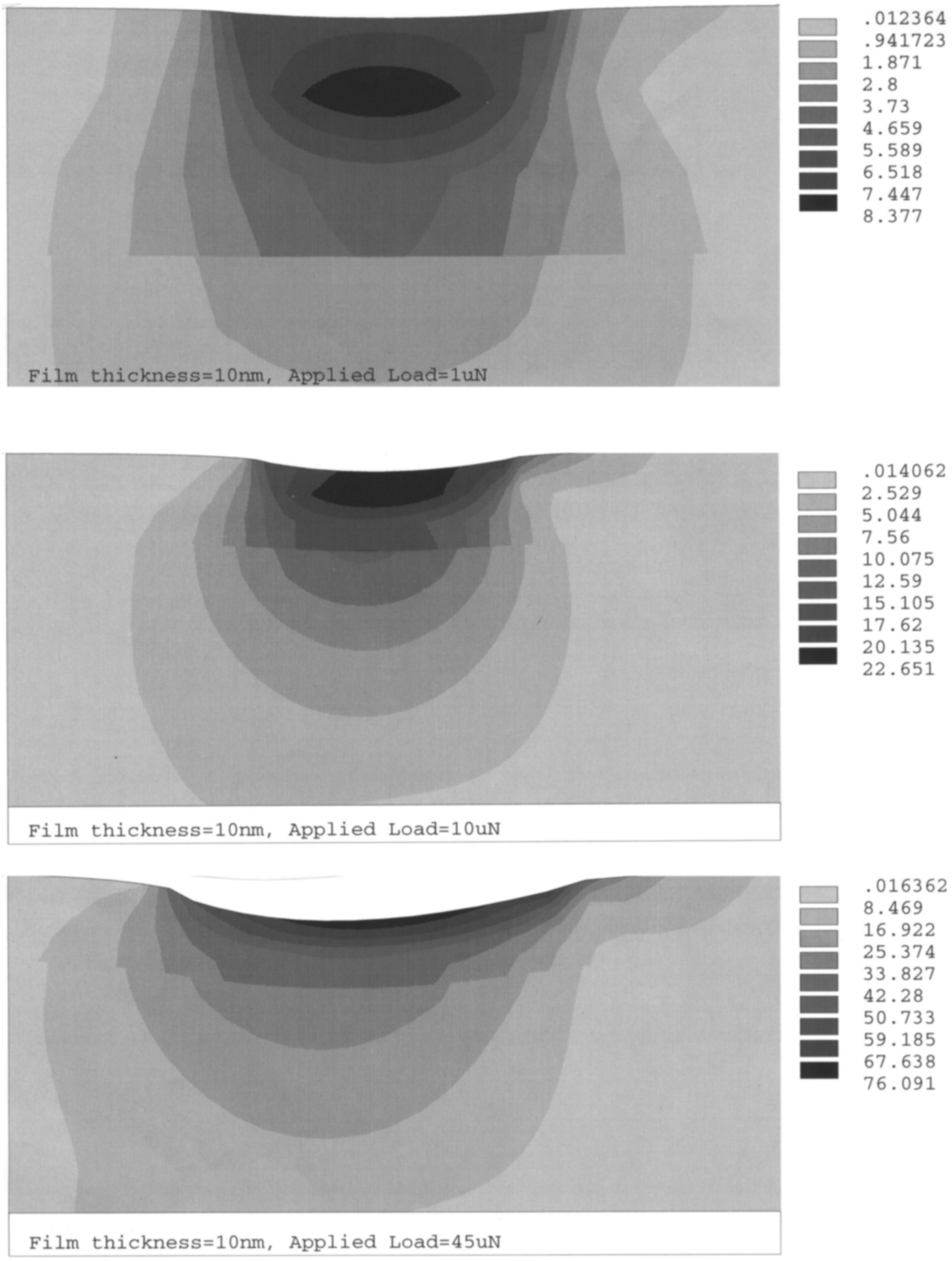

Fig. 10. Contours of von Mises equivalent stress of the deformed 10 nm CN_x coating when it slid against a diamond pin under applied loads of 1 μN (up), 10 μN (middle) and 45 μN (bottom), respectively. The abrupt variation of contours indicates the position of the CN_x/substrate interface. The numbers near the labels indicate the values of von Mises equivalent stress in units of GPa.

Acknowledgements

This work is supported by the Japanese Society for Promotion of Science (JSPS). The authors would like to thank Drs L. Zhou and K. Adachi for their help in the fabrication of the thin coating.

References

[1] G. Binnig, S.F. Quate, C. Gerber, Phys. Rev. Lett. 56 (9) (1986) 930–933.
[2] C.M. Mate, G. MaClelland, R. Erlandsson, S. Chiang, Phys. Rev. Lett. 59 (17) (1987) 1942–1945.

[3] R. Kaneko, T. Miyamoto, E. Hamada, Adv. Info. Storage Syst. 1 (1991) 267–277.
[4] R. Kaneko, S. Oguchi, T. Miyamoto, Y. Andoh, S. Miyake, STLE Special publication SP-29, 1990, p. 31–24.
[5] B. Wei, K. Komvopoulos, J. Tribol. 118 (1996) 431–438.
[6] E.V. Anoikin, G.S. Ng, M.M. Yang, J.L. Chao, J. Elings, D. Brown, IEEE Trans. Magn. 34 (4) (1998) 1717–1719.
[7] A. Khurshudov, M. Olsson, K. Kato, Proc. Int. Tribo. Conf. Yakohama, 1995, pp. 1937–1942.
[8] D. Beeman, J. Silverman, R. Lynds, M.R. Anderson, Phys. Rev. B30 (1984) 870.
[9] User operation manuals, 2nd version, Seiko Instruments Inc, Japan, 1998.
[10] J. Ruan, B. Bhushan, ASME J. Tribol. 116 (1994) 378–388.
[11] E.C. Cutiongca, D. Li, Y.W. Chung, C.S. Bhatia, J. Tribol. 118 (1996) 543.
[12] K. Kato, M.W. Bai, N. Umehara, Y. Miyake, Surf. Coat. Tech. 113 (3) (1999) 233–241.
[13] Y. Andoh, R. Kaneko, Proc. Int. Tribo. Conf., Yakohama, Japan, 1995, p. 1913.
[14] L.G. Hector, S.R. Schmid, Wear 215 (1998) 247–256.
[15] C.M. Mate, G.M. McClelland, R. Erlandsson, S. Chiang, Phys. Rev. Lett. 59 (17) (1987) 1942–1945.
[16] R. Kaneko, S. Umehara, M. Hirano, Y. Andoh, T. Miyamoto, S. Fukui, Wear 200 (1996) 296–304.
[17] B. Wei, B. Zhang, K.E. Johnson, J. Appl. Phys. 83 (5) (1998) 2491–2499.
[18] D.P. Hess, A. Soom, Unsteady friction in the presence of vibrations, in: I.L. Singer, H.M. Pollock (Eds.), Fundamentals of Friction: Macroscopic and Microscopic Processes, Kluwer Academic Publishers, Dordrecht, 1992, pp. 535–552.
[19] M. Scherge, J.A. Schaefer, Tribol. Lett. 4 (1998) 1.
[20] T.W. Scharf, R.D. Ott, D. Yang, J.A. Barnard, J. Appl. Phys. 15 (1999) 3142–3154.
[21] Z. Jiang, C.J. Lu, D.B. Bogy, C.S. Bhatia, T. Miyamoto, Thin Solid Films 258 (1995) 75–81.
[22] K. Hokkirigawa, K. Kato, Tribo. Int. 21 (1988) 51–57.
[23] I.L. Singer, H.M. Pollock, Fundamentals of friction: macroscopic and microscopic process, NATO ASI Series 220, Kluwer Academic Publishers, Boston, 1992, p. 533.
[24] A.V. Kulkarni, J.T. Wyrobek, Z. Qian, J.M. Siversten, J. Judy, Mater. Res. Soc. Symp. Proc., 505, Thin-Films-Stresses and Mechanical Properties VII, 1998, pp. 217–222.
[25] H. Deng, T.W. Scharf, J.A. Barnard, J. Appl. Phys. 81 (8) (1997) 5396–5398.
[26] J.C. Hay, A. Bolshakov, G.M. Pharr, J Mater. Res. 14 (1999) 2305–62296.
[27] W.C. Oliver, G.M. Pharr, J. Mater. Res. 7 (1992) 1564.
[28] G.M. Hamilton, L.E. Goodman, J. Appl. Mech. 88 (1966) 371–376.
[29] E.R. Kral, K. Komvopoulos, D.B. Bogy, J. Appl. Mech. 62 (1995) 29–42.
[30] K.L. Johnson, Contact mechanics, Cambridge University, 1984, UK.
[31] S. Sriram, B. Bhushan, Wear 217 (1998) 251–261.